Research on Engineering Structures & Materials
www.jresm.org
MIM Research Group

Research Article

Torsional ductility and toughness of reinforced concrete beams with a new method of splice remedy

Ziadoon M. Ali [*,a], Akram S. Mahmoud [b]

Department of Civil Engineering, University of Anbar, Ramadi, Iraq

Article Info

Article History:

Received 13 Oct 2025

Accepted 24 Nov 2025

Keywords:

Torsional ductility;
Toughness;
Lap splice;
Bond strength;
Experimental study

Abstract

This study investigated the torsional performance of reinforced concrete (RC) beams using spliced reinforcement bars. Inadequate lap splice lengths were specifically employed to investigate the influence of diminished splice length on torsional capacity, torsional ductility, and torsional toughness. Insufficient splice lengths are especially important in practice, since increasing splice length in FRP-reinforced structures elevates material cost, while excessively splices may lead to reinforcement congestion that restricts adequate concrete placement. A new splice strengthening approach utilizing Carbon Fiber Reinforced Polymer (CFRP) sheets was implemented, applied transversely around the splice zone and covered with resin to enhance confinement and improved bond strength. The novelty of this study resides in the new CFRP configuration developed to strengthen inadequate lap splices of GFRP bars under pure torsion, a condition not previously investigated in comparison to flexural and shear loads. Seven RC beams were fabricated, cast tested under pure torsion to examine the effects of splice length, CFRP strengthening, and stirrup spacing. Results indicated that the shortest substandard splice affected torsional capacity by approximately 36.45%, while torsional ductility and toughness were reduced by up to 36.76% and 70.7%, respectively, in comparison to a beam with continuous bars. Extending stirrup spacing from 100 to 150 mm reduced torque by 15% while significantly impacting ductility. The strengthening of CFRP significantly improved ultimate torque capacity, torsional ductility, and toughness. Finally, this transverse wrapping technique may offer practical on-site benefits, as its enhanced confinement may allow minimizing the required splice length while preserving acceptable torsional performance, and it can be applied manually without required instruments compared to other methods, including welding and couplers.

1. Introduction

Reinforced concrete (RC) structures generally require bar splicing to address construction problems or fabrication considerations [1,2]. While traditional steel reinforcement splicing has been well investigated, the performance of spliced glass fiber reinforced polymer (GFRP) bars exists currently insufficiently studied, specifically under torsional load conditions. GFRP reinforcement has advantages include corrosion resistance and a superior strength-to-weight ratio [3,4]; however, its distinct mechanical properties need careful consideration at splice regions. Inadequate lap splice lengths in GFRP-reinforced beams may result in premature failure when subjected to torsional loads.

The structural response of reinforced concrete members to torsion has garnered more attention owing to the rising utilization of torsion-sensitive components, including spiral slabs and curved bridge girders. Torsion is highly associated with bending and shear stresses, and eccentric loads

*Corresponding author: zaydon88@uoanbar.edu.iq
[a]orcid.org/0000-0002-8114-0990; [b]orcid.org/0000-0002-1956-0281
DOI: http://dx.doi.org/10.17515/resm2025-1253ic1013rs

make torsion an important consideration in bridge design [5–7]. Prior studies have investigated the performance of reinforced concrete beams with transverse and longitudinal glass fiber reinforced polymer reinforcement subjected to torsion. Shehab et al. [8] investigated FRP-RC beams subjected to simultaneous bending and torsion, discovering that GFRP stirrups failed prior to the crushing of the concrete cover due to inadequate bonding. Deifalla [9] presented adhesively bonded GFRP stirrups, which enhanced ultimate torque relative to bent stirrups.

Mohamed et al. [10] examined concrete beams reinforced with sand-coated GFRP and CFRP bars subjected to pure torsion, demonstrating that beams with minimal transverse reinforcement failed due to the fracture of FRP stirrups, while those with elevated transverse reinforcement ratios failed due to concrete crushing in diagonal struts. These results highlight the essential importance of transverse reinforcement while indicating that inadequate lap splice length in longitudinal FRP bars, which withstand torsional loads post-concrete cracking, is a mainly neglected concern. Previous research attempted to fix splice defects by adding resin to the splice region and longitudinally wrapping the bars with CFRP sheets [11–16]. The method enhanced tensile strength and is simpler to perform than conventional techniques such as couplers or welding [15], but it provides limited enhancement in bond behavior, especially under overloading conditions.

This work presents a new configuration of transverse CFRP wrapping, wherein CFRP sheets wrap perpendicularly and directly around the spliced bars. This method aims to improve resistance to bar slide and develop the bond-transfer mechanism between steel and concrete under rotational loads. This research evaluates the performance of the suggested splice-strengthening approach under pure torsion, measuring its influence on ultimate torque capacity, torsional ductility, and toughness, in contrast with prior studies that mainly focused on flexural behavior.

This study aims to investigate the effect of inadequate lap splice length on the torsional behavior of reinforced concrete beams and to assess the performance of transverse CFRP wrapping as a suitable strengthening technique. The scope includes experimental testing of seven beams subjected to pure torsion, which includes differences in splice length, CFRP usage, and stirrup spacing.

2. Experimental Program

2.1 Materials

The experimental program utilized Ordinary Portland Cement (Type I) as the primary binder. Naturally graded sand served as the fine aggregate, while crushed gravel with a maximum nominal size of 10 mm was used as the coarse aggregate. Clean potable water, free from impurities, was employed for both mixing and curing the concrete specimens. To improve the workability during casting, a superplasticizer (Visco Crete 225 S) was added to the concrete mix. All materials were sourced locally and complied with the relevant standard specifications for concrete production. Cylindrical specimens measuring 150×300 mm was cast and tested, achieving an average compressive strength of about 49.5 MPa. The details of the materials and their weights per cubic meter are presented in Table 1, while (Fig. 1) illustrates the casting and curing processes. The mechanical properties of the reinforcing materials used in the study are summarized in Table 2.

Table 1. Concrete components

Components	Quantity
W/C: Water/cement Ratio (%)	28
Superplasticizer (Visco crete 225 S) (Liter/m^3)	5
Water (kg/m^3)	140
LocalCement (kg/m^3)	500
Local crushed gravel (kg/m^3)	1060
Local natural sand (kg/m^3)	710

Table 2. Mechanical properties of reinforcement

material	Bar diameter (mm)	Area (mm^2)	Yield strength (MPa)	Tensile ultimate strength (MPa)	Elastic modulus (MPa)
Steel bars	8	28	422	460	200000
GFRP bars	10	78.5	-----	1024	45000

Fig. 1. Casting and curing of beams

2.2 Splice Remedy

The present research used unidirectional CFRP sheets (Type: SikaWrap®-300 C) with fibers oriented at 0°. The manufacturer specifies that the dry fiber tensile strength is 4,000 N/mm^2 and the dry fiber modulus of elasticity is 230,000 N/mm^2, according to the information in the manufacturer's technical data sheet (ISO 10618). (Fig. 2) illustrates that the CFRP sheet was fabricated as a plane sheet and subsequently coated with a 1 mm layer of Sika Dur 330 resin for effective bonds to the spliced bars.

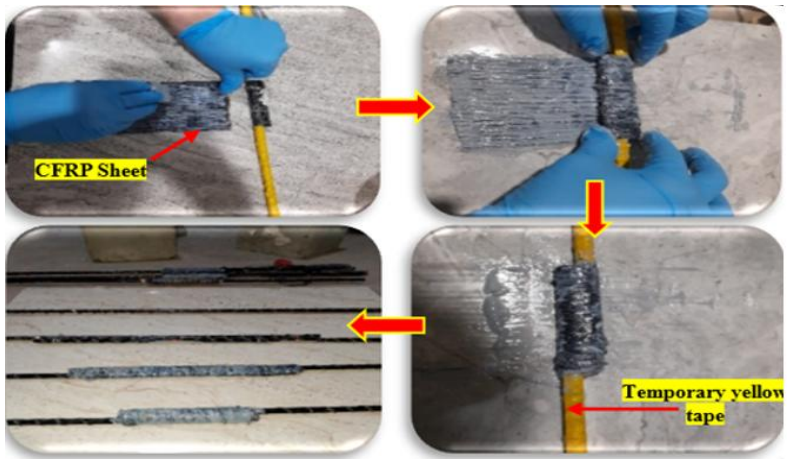

Fig. 2. Splice region remedy by CFRP sheet

The CFRP sheet was subsequently wrapped in transverse direction surrounding the spliced bars region in two layers to ensure an adequate anchorage. The width of CFRP coincided with the length of the splice region (i.e., 100 and 200 mm).In contrast to the prior method [11-13], which involved longitudinally wrapping the CFRP sheet around the spliced bars, the objective of the current new technique of transverse CFRP sheet wrapping is to achieve effective confinement around the substandard lap splice region. The existing method may resist slippage better and elevate the tensile stresses in the spliced bars, potentially attaining yield strength, while also allowing the specimen to endure a greater load and avoid splitting failure. Figure 2 illustrates the wrapping

technique and different lap splice configurations. Fig. 3 and 4 illustrates the specifications of reinforced beams and splice position with details, respectively.

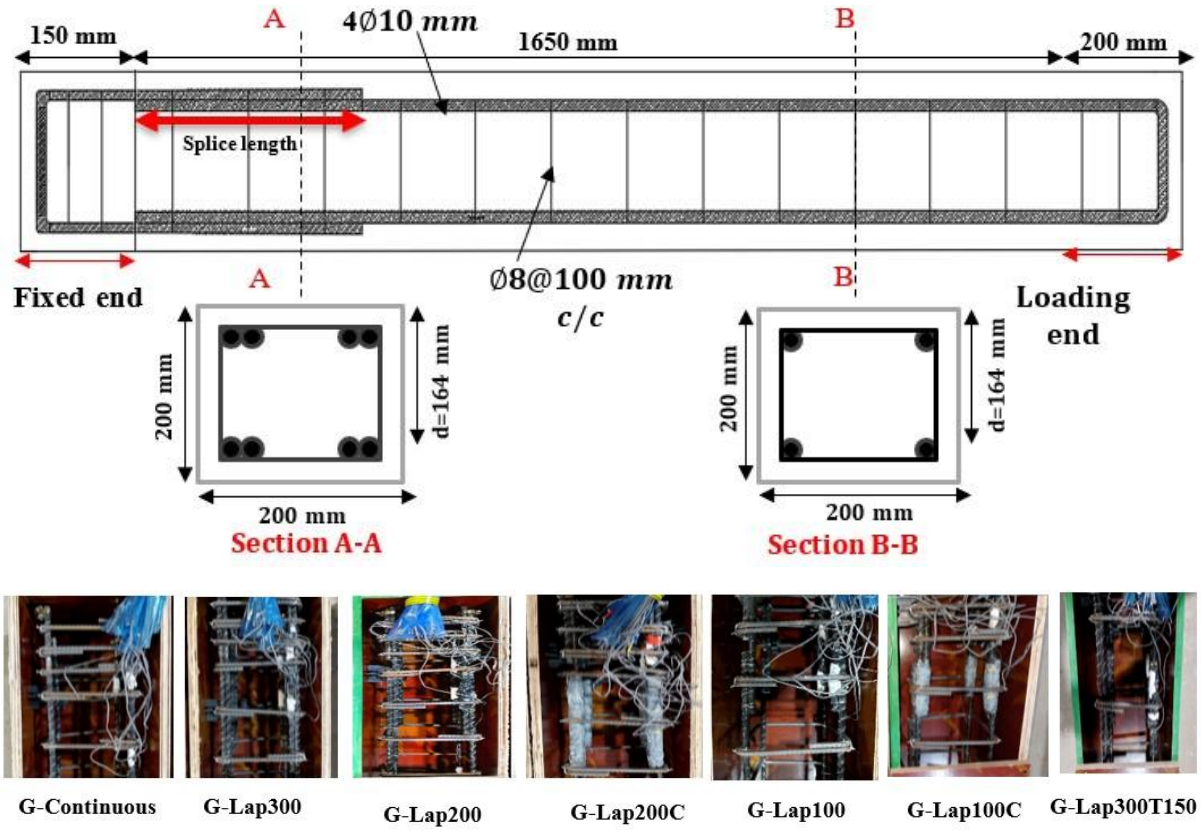

Fig. 3. The specifications of reinforced beams

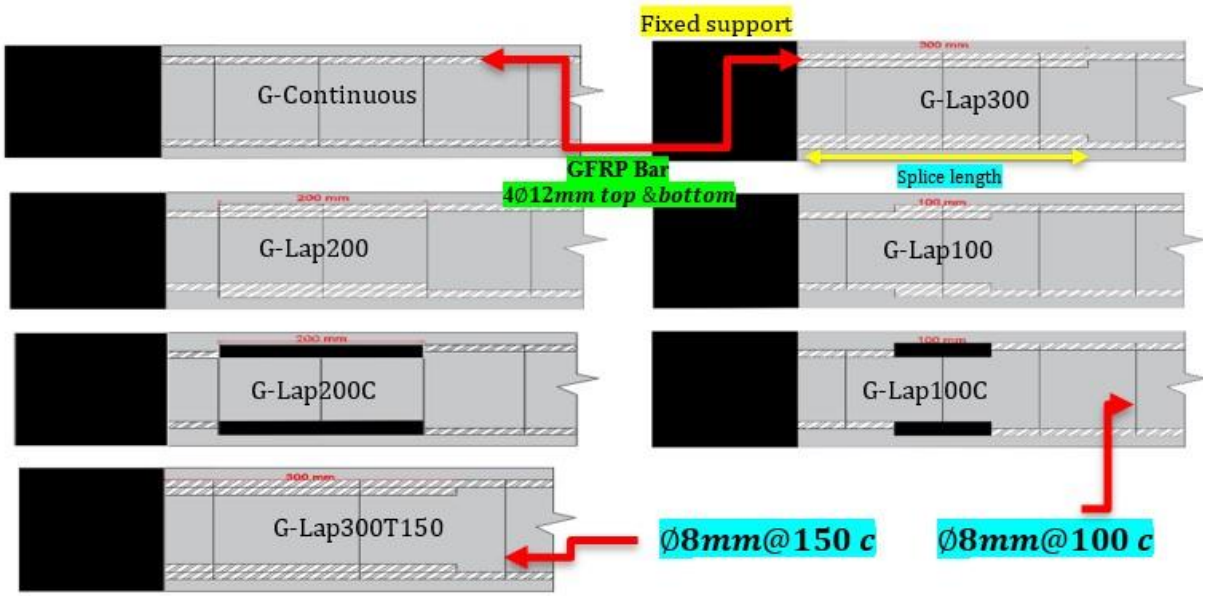

Fig. 4. The details of splice position near the fixed support

2.3 Beams Fabrication

Seven reinforced concrete beams were manufactured, cast, and subjected to pure torsion tests. As shown in (Fig. 3), the beam measurements were 200 x 200 mm with an overall span of 2000 mm (1650 mm effective span). 4Ø10 mm GFRP bars reinforced the beams in the longitudinal direction. All specimens were reinforced with Ø8 at 100 mm in the transverse direction except one beam, which was reinforced by Ø8 mm at 150 mm as a parameter. The parameters included the presence

of a splice bar and the lap splice length, which ranged between 300 mm and 100 mm to obtain a substandard length. The inadequate lap splices of lengths 200 mm and 100 mm were strengthened with CFRP sheets and Sika Dur 330 resin. These were then compared to the inadequate lap splices that had not been strengthened. Table 3 presents the details of the parametric study.

2.4 Test Setup

A 500-kN universal test machine was set up for testing all reinforced concrete beams. (Fig. 5) and (Fig. 6) illustrate the test configuration and provides a schematic 2D representation of the testing equipment. The testing equipment comprises two supports. The first support is a fixed support, while the subsequent support is a movable support for applying load. The load was applied vertically, linked to the beam made of steel used as arm to produce pure torque as illustrated in (Fig. 5) (Fig. 6). From (Fig. 5), the steel shaft allows only for rotation, and the vertical movement was prevented to avoid the effect of shear and bending moment. An electromechanical transducer was employed to transform rectilinear motion into an electrical Signal. Three linear variable differential transducers (LVDTs) were employed to measure the displacement with a capacity of 120 mm after being linked to an electronic data logger. The LVDTs were previously calibrated to ensure reliable reading of twisting angle.

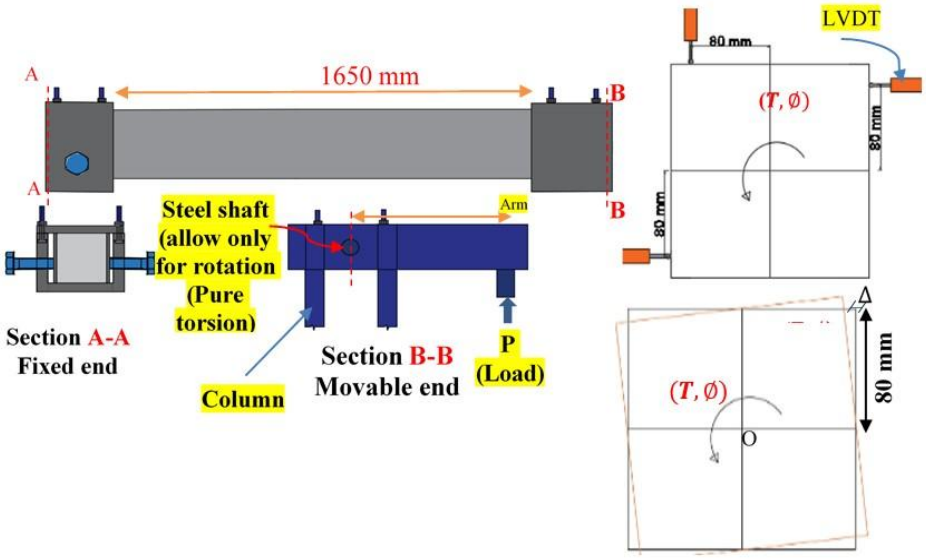

Fig. 5. Schematic diagram for test setup

The LVDTs were positioned on the movable end from the side of applied torque to measure the maximum displacement of the specimen. The position of the LVDTs is illustrated in (Fig. 5) and (Fig. 6). The angle of twist due to applied torque (T) can be found from eq (1) as follows:

$$\emptyset = tan^{-1}(\frac{\Delta}{80\ mm}) \quad (1)$$

Where Δ: Displacement recorded from the LVDTs in mm, 80 mm: Distance from the LVDTs position to the point O as shown in Fig. 6.

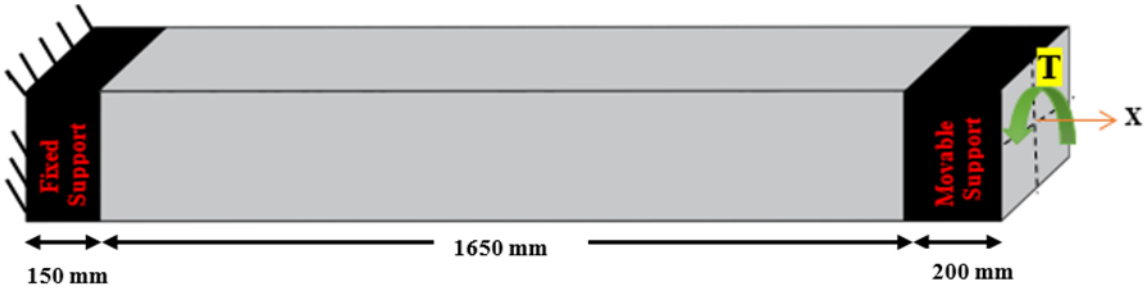

Fig. 6. Experimental testing setup

The load was incrementally applied from zero until failure resulted and the displacement was recorded at each 0.5kN increment. An experimental assessment measured the ultimate torque and torque-angle twist curve. From the torque-twisting angle curves, the torsional ductility and toughness were computed and discussed.

3. Results and Discussion

The results including values and load deflection curve of the tested beams were illustrated in (Fig. 7) and Table 4.

3.1 Ultimate Torque

Table 4 and (Fig. 7) illustrate the ultimate torque capacity for the specimen. The ultimate torque and twist angle at the moveable end decreased as the splice length decreased, particularly in cases where the lap splice length was substandard. Specifically, the G Lap300's ultimate torque capacity decreased by 14% compared to the G-Continuous. It indicates that the G-Lap 300 lacks lap splice length.

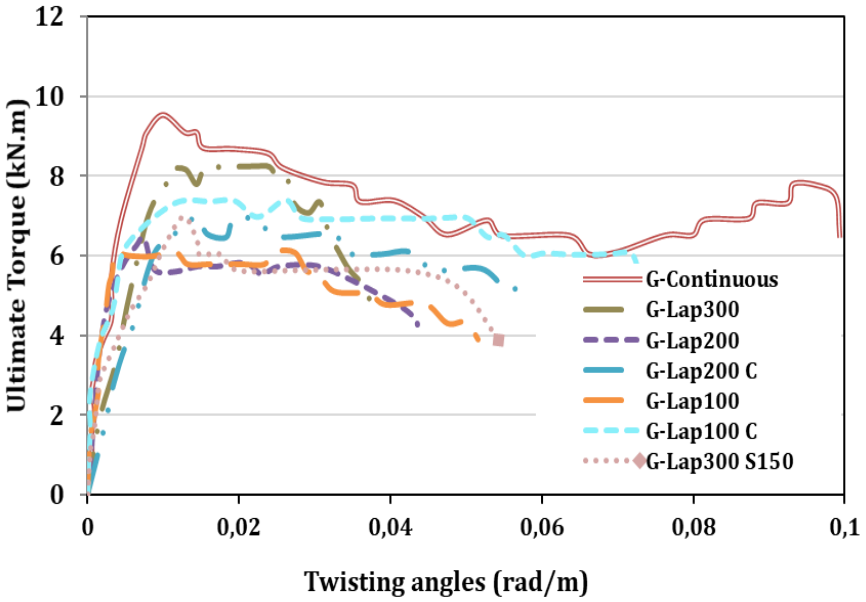

Fig. 7. Torque-Twisting angle curves

The reduction in ultimate torque capacity is minimal compared to the decline in ultimate load capacity under flexural loading, where the decrease in ultimate load has reached 40% with the

same length of splice length and the same type of GFRP reinforcement [13]. This may be an indication that the short lap splice length could cause the ultimate capacity to drop significantly when flexure and torsion loads are applied simultaneously. The ultimate torque capacity declined by 33% and 36% compared to the reference beam with continuous GFRP bars when the lap splice was shortened by 33.33% for beam G Lap 200 and 67.667% for beam G Lap 100. Insufficient lap splice length may cause weak stress transfer between spliced bars, reducing bonding stresses. Fig. 8 shows how splice length affects G-Group torque capacity.

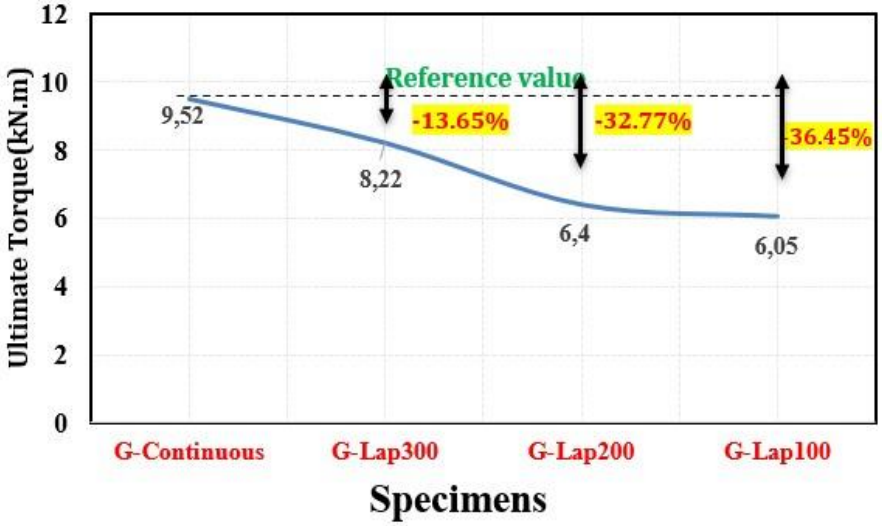

Fig. 8. Effect of unstrengthen lap splice length on ultimate torque capacity

Table 3. Details of the parametric study

Specimens	Description of reinforcement with splicing		Splice length /Ls (mm)	Splice Configuration
	Longitudinal	Stirrups		
G-Continuous	4Ø10 mm Continuous GFRP bar	ø8mm@100mmc/c	Continuous	
G-Lap300	4Ø10 mm GFRP with 300 mm lap splice length		300	
G-Lap200	4Ø10 mm GFRP with 200 mm lap splice length		200	
G-Lap200C	4Ø10 mm GFRP with 200 mm lap splice length and CFRP remedy/1ply		200	
G-Lap100	4Ø10 mm GFRP with 100 mm lap splice length		100	
G-Lap100C	4Ø10 mm GFRP with 100 mm lap splice length and CFRP remedy		100	
G-Lap300 T150	4Ø10 mm GFRP with 300 mm lap splice length	ø8mm@150mmc/c	300	

The strengthening method for substandard 100 mm and 200 mm lap splice lengths was tested under ultimate torque capacity. Strengthening increased ultimate torque capacity and angle of twist. The G-Lap200C specimen had 8% more ultimate torque than the G-Lap200. Significantly, as shown in (Fig. 9), the ultimate torque capacity increased by 21% for G-Lap100C compared to G-Lap100 when the strengthening method was applied to the substandard lap splice length of 100 mm. The G-Lap200C had 84.3% torque capacity and the G-Lap100C 86.4% compared to the 300 mm lapping length reference beam (G-Lap300). Results show that CFRP strengthening compensates better for decreased lap length in shorter sizes, indicating that CFRP wrapping

improves bond characteristics, potentially reducing splice lengths while maintaining torsional resistance.

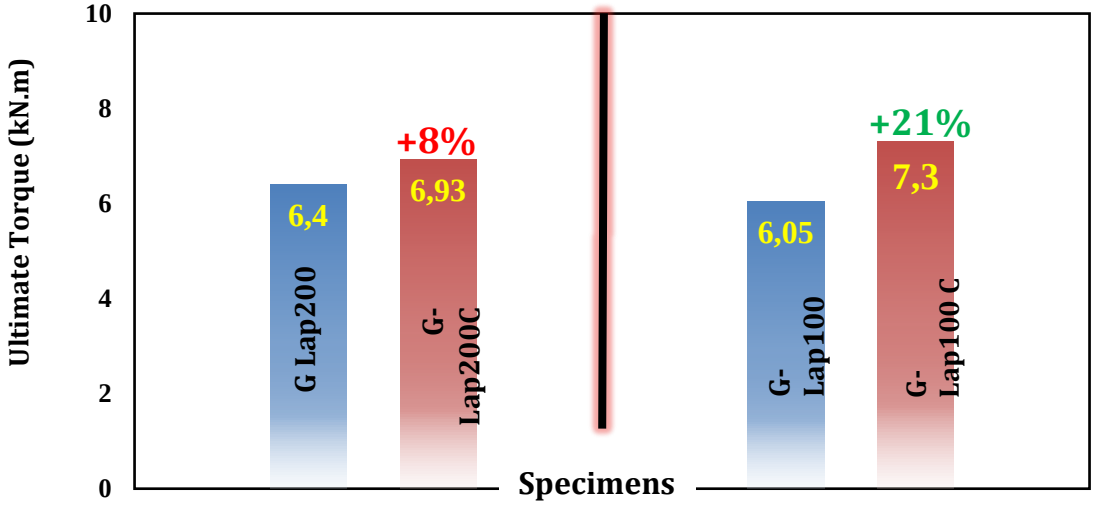

Fig. 9. Effect of splice remedy on the ultimate torque capacity for G-Group

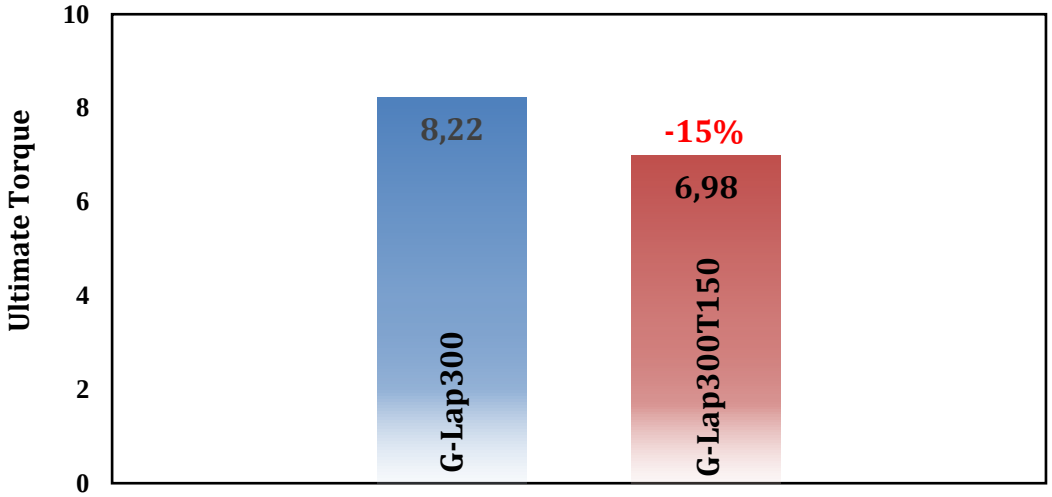

Fig. 10. The effect of transverse reinforcement on splice region

Table 4. Results of tested specimens

Group	No.	Specimen	T_{cr}	$\emptyset_{cr}$	T_u	Difference in T_u (%)	$\emptyset_u$	Difference in $\emptyset_u$ (%)
G-group	1	G-Continuous	8.00	0.0062	9.52	Reference	0.0100	Reference
	2	G-Lap300	7.50	0.0090	8.22	-13.65[a]	0.0130	+30.00[a]
	3	G-Lap200	6.12	0.0050	6.40	-32.77[a]	0.0074	-26.00[a]
	4	G-Lap200C	6.10	0.0048	6.93	+8.3[b]	0.0380	+413.50[b]
	5	G-Lap100	5.70	0.0033	6.05	-36.45[a]	0.0048	-52.00[a]
	6	G-Lap100C	6.25	0.0047	7.30	+20.66[c]	0.0130	+170.80[c]
	7	G-Lap300-T150	5.97	0.0091	6.98	-15[d]	0.0126	-3.08[d]

Where T_{cr}: Cracking Torque (kN.m); $\emptyset_{cr}$: Twist angle at cracking stage (rad/m); T_u: Cracking Torque (kN.m); $\emptyset_u$: Twist angle at ultimate stage (rad/m); a: compared to G-continuous; b: compared to G-Lap200; c: Compared to G-Lap100; d: compared with G-Lap300.

The effect of spacing of stirrups was also investigated in terms of ultimate torque capacity. The spacing stirrups were 100 mm for the G-Lap300 specimen. As shown in Table 4 and (Fig. 10), the increasing of spacing to 150 mm to get G-Lap300 T150, the ultimate torque capacity, decreases by 15%. This may be due to a lack of a confinement ratio of steel stirrups near the splice region as well as the loss of certain transverse ratios that play a significant role in resisting applied torque. The ultimate twist angle was not significantly affected by the reduction in transverse ratio, as the ultimate angle of twist decreased by only 3.08% when the spacing was increased to 150 mm to obtain G Lap300 T150.

3.2 Ductility Index

Ductility is an important material feature that enables plastic deformation and energy absorption avoiding catastrophic collapse. It indicates a material's capacity to resist applied pressure post-yielding without sudden failure. The method of measurement provided by Chao et al. [17] has been extensively employed. The ductility index (μ_E) supports the energy-based method, since it measures the ability to absorb energy, represented as the ratio of total energy to elastic energy, as follows Eq (2) [13]:

$$\mu_E = 0.5\ (\frac{E_t}{E_e} + 1) \tag{2}$$

In (Fig. 11), μe represents ductility indices; Ee represents elastic energy (area below slope S), and Et represents total energy (area under load-deflection curve up to failure load). This method also works for torque-angle twist curves. Table 5 shows the energy approach ductility indices as well as torsional toughness of all tested specimens. The Slope S is calculated from Eq(3).

$$S = \left(\frac{P1*S1+(P2-P1)S2}{P2}\right) \tag{3}$$

Where P_1, S_1, P_2, S_2, and S are illustrated in Fig.11.

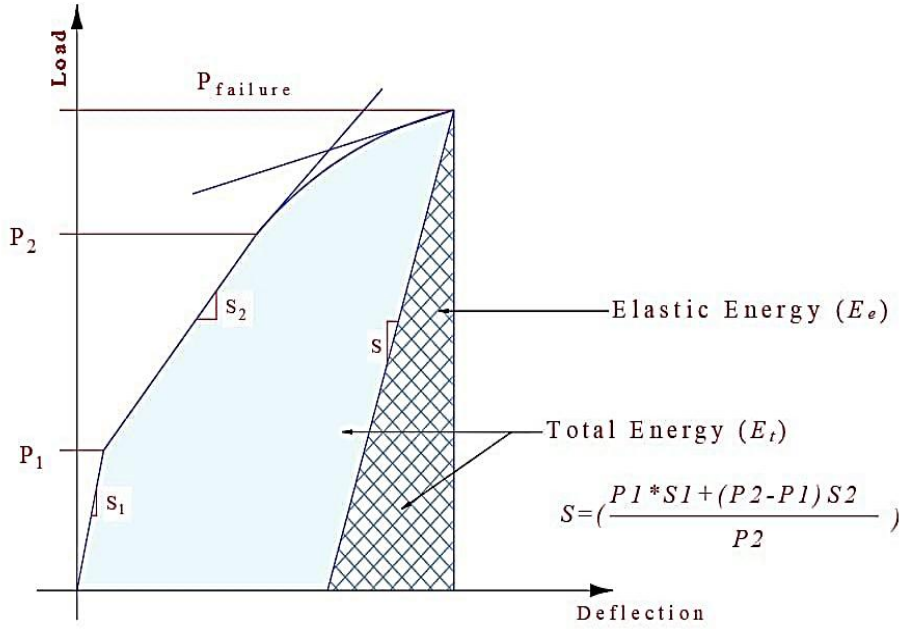

Fig. 11. Energy method for ductility calculation

Ductility index values are shown in Table 5. The 300 mm (30db) lap splice length has minimal impact on ductility index. Table 5 shows that G Lap 300 has 9.31% less ductility than G-continuous. The ductility index dropped by 36.76% and 26.47%, respectively, compared to a reference beam with continuous bars (G-Continuous) and by 30.3% and -18.92% compared to G-Lap 300, when the lap splice length was reduced to 20 d_b and 10 d_b, respectively. A shorter lap splice length reduces the anchoring length, which may cause slip or failure at the splice region, limiting the beam's plastic

deformation and energy absorption, reducing ductility. The new lap splice method improved the ductility index. Table 5 shows that the G-Lap200C specimen had a 155% higher ductility index than the G-Lap200. When the strengthening technique was used on the inadequate lap splice length of 100 mm (10 db), G Lap100C had 165.34% better ductility than G Lap100, as shown in Table 5.

Table 5. Ductility index for all test specimens

No.	Specimen	E_e	E_t	$\mu = \frac{1}{2}(\frac{E_T}{Ee} + 1)$	Difference in ductility (%)	Toughness kN.m×rad/m×10^{-3}	Difference in Toughness (%)
1	G-Continuous.	22.01	68.00	2.04	**Reference**	716	Reference.
2	G-Lap300	22.50	61.00	1.85	-9.31[a]	248	-65.40[a]
3	G-Lap200	19.00	30.00	1.29	-36.76 [a]	234	-67.32 [a]
4	G-Lap200C	40.40	225.30	3.29	+155.04[b]	327	+40.00[b]
5	G-Lap100	9.98	20.00	1.50	-26.47[a]	210	-70.70[b]
6	G-Lap100C	11.80	82.12	3.98	+165.34 [c]	470	+123.00[c]
7	G-Lap300-T150	22.40	58.40	1.80	-2.70 [d]	266	+7.25[d]

Where a: compared to G-continuous; b: compared to G-Lap200; c: Compared to G-Lap100; d: compared with G-Lap300

This may be attributed to the fact that CFRP strengthening around spliced bars improved reinforcement bar strain and stress resistance, delaying brittle failures. This increases beam deformation before failure, resulting in improved specimen ductility. Table 5 also illustrates that extending the stirrups spacing from 100 mm to 150 mm to obtain the G-Lap300 T150 beam resulted in a very slight decrease in ductility, a 2.7% reduction in ductility compared to G-Lap300.

3.3 Torsional Toughness

Toughness defines a material's capacity to absorb energy prior to fracturing. The torsional toughness values were calculated from the area under torque-twisting angle curves. Table 5 shows all tested beams' torsional toughness. The G-continuous beam has the highest toughness value. Lap splice lengths of 300, 200, and 100 mm reduce torsional toughness by 65.4, 67.32, and 70.7%, respectively, compared to G-continuous. G Lap200 had a torsional toughness of 234, while G Lap200C had 327 thanks to lap spliced GFRP bars wrapped in CFRP sheet and coated with resin. CFRP wrapping increases toughness by 39.7%, as shown by the differential ratio of G Lap200C to G Lap200. G Lap100 had lap splice GFRP bars length 100 mm with a torsional toughness of 200, while G Lap100C had CFRP-wrapped, resin coated bars with 470.G Lap100C has 124% higher torsional toughness than G Lap100. The CFRP wrapping may increase the toughness of G Lap200C and G Lap100C by strengthening the splice region, strengthening the bond between the two GFRP bars, and increasing the beams' torsional resistance. By preventing reinforcement bar and concrete slip, CFRP confinement may increase torsional toughness, especially at the lap splice. This provides enhanced load transfer and ensures the integrity of the reinforcement under stresses due to torsional loads. Furthermore, CFRP enhanced ductility, enabling the structure to experience increased plastic deformation prior to failure. The integration of improved stress transfer and higher ductility effectively improves energy absorption under torsion, resulting in superior torsional toughness.

For the variation in transverse reinforcement ratio, the 150 mm stirrup spacing specimen (G-Lap300T150) had a torsional toughness of 266, while the 100 mm stirrup spacing specimen (GLap300) had 248. Reduced transverse reinforcement ratio improves torsional toughness by 7.25% as shown in Table 5. The wider stirrup spacing in GFRP-reinforced specimens may be enabling a more efficient stress distribution within the lap splice region. When stirrups are closely spaced (100 mm), the confined condition may concentrate stresses at specific locations along the spliced GFRP bars, and then the GFRP bars demonstrate brittleness properties, resulting in potential regional bond failures that decrease overall torsional toughness.

4. Crack Pattern

Assessing the mode of failure is essential for identifying the governing failure mechanism [18]. The crack pattern and results are presented in (Fig. 12) and Table 6. The crack pattern was affected by the presence of lap splice region. (Fig. 13) illustrates the combination of torsional cracks as well as splitting cracks (longitudinal and transverse cracks) concentrated within splice region.

Table 6 illustrates that the beam reinforced having continuous GFRP bars (G-Continuous) demonstrated a helical crack mode reaching over more than half of the span of the beam, indicative of the common torsional response of unsliced parts. nevertheless, with the producing of the splice, cracks may became more concentrated within splice zone, as shown in Figure 11, which may be related to localized bonding stresses and partial slipping between the spliced bars. This concentration might have diminished the overall crack length but resulted in marginally wider cracks. When CFRP sheets were directly wrapped around the spliced bars (i.e. G-Lap200C and G-Lap100C specimens), the enhanced confinement may have reduced bar slipping and cracking progression, perhaps leading to a reduction in cracking width approximately 33–55% as shown in Table 1. These results might reflect an enhancement in bond stress distribution and torsional strength.

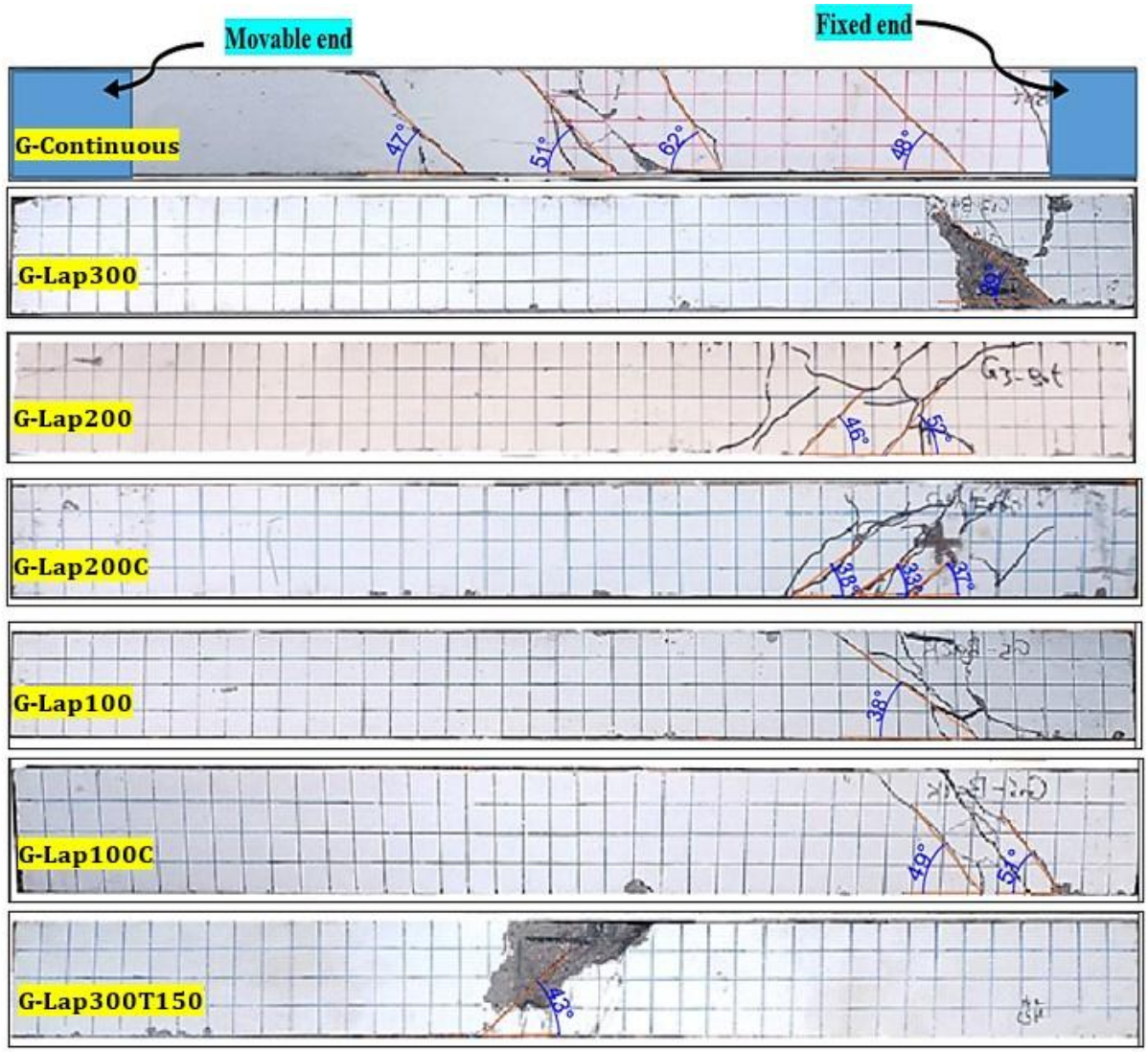

Fig. 12. Crack patterns for test specimens(one face comparison)

Fig. 13. Cracks types within splice region(G-Lap300)

Table 6. Crack results

Specimen	Maximum Crack width (mm)	Difference in crack width (mm) (%)
G-Continuous.	2.77	Ref.
G-Lap300	4.30	+55[a]
G-Lap200	4.50	+62.5[a]
G-Lap200C	2.00	-55.5[b]
G-Lap100	3.00	+8.3[a]
G-Lap100C	2.00	-33.3[c]
G-Lap300-T150	4.40	+2.3[d]

Where; a: compared to G-continuous, b: compared to G-Lap200, c: Compared to G-Lap100 and d: compared with G-Lap300

The enhancement in crack pattern, ultimate torque and torsional ductility might be linked to multiple interaction reasons. The CFRP confinement may have improved the bond stress distribution along the splice, minimizing localized splitting and delaying bar slip. The transverse wrapping may have contributed lateral confinement in the splice zone, perhaps enhancing stress transfer quality between the bars and the surrounding concrete. Thus, this improved confinement may have permitted the beams to resist greater torque and shown higher post-cracking ductility.

5. Torsional Strength Verification

The ultimate torque capacity was calculated theoretically using the provision of ACI318-19 because of the transverse reinforcement is made of steel and play a main role in torsional strength compared to longitudinal GFRP. The equation of ultimate strength is as follow:

$$T_n = \frac{A_t}{S} \times f_{yt} \times 2A_\circ \, cot\theta \tag{4}$$

Where; T_n: Nominal torsional strength *[kN·m]*, A_t : Area of stirrups reinforcement *[mm²]*, S: Spacing of stirrups *[mm]*, f_{yt}: Yield strength of stirrups reinforcement *[MPa]*, $A_\circ$: Area enclosed by the shear flow path (effective torsional area) *[mm²]*= $X_\circ * Y_\circ$, θ: Angle of diagonal compression (crack angle) *[degrees]*. θ Assumed to be 45°(for design consideration).

(Fig. 14) and table 7 illustrates the details of cross section geometry that is require for determination of torsional strength.

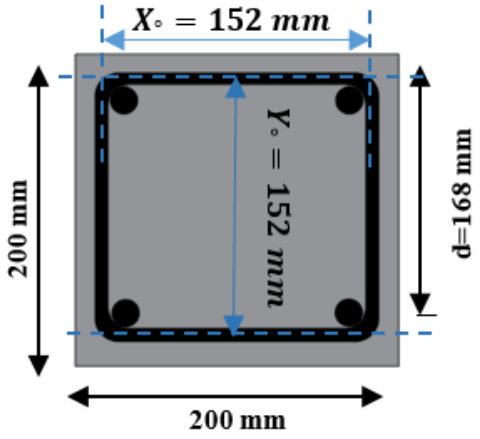

Fig. 14. Cross sectional beam

Table 7. Geometrical details of cross-sectional beam

Property	Value
b (beam width)	200 mm
H(beam height)	200 mm
Effective depth	164mm
Clear cover	20mm
$X_\circ$ (horizontal distance for center to center of two legs of stirrups	152 mm
$Y_\circ$ (vertical distance for center to center of two legs of stirrups	152 mm
$A_{\circ_h} = X_\circ * Y_\circ$	23104 mm^2
$A_\circ = 0.85\ A_{\circ_h}$	19638.4

- Ø8 mm for stirrups: Abar = 50.26 mm2 and stirrup spacing =100 mm for all specimens except the G-Lap300T150
- For one leg of stirrups $\frac{A_t}{S} = \frac{50.26}{100} = 0.5026\ mm$
- Assume $\theta = 45°$
- $T_n = \frac{A_t}{S} \times f_{yt} \times 2A_\circ\ cot\theta$ =0.5026× 422 × 2 × 19638.4 × 1 × 10^{-6} = 8.33 $kN.m$
- According to ACI318-19 the ultimate torque is 8.33 kN.m
- For S=150, for one leg of stirrups $\frac{A_t}{S} = \frac{50.26}{150} = 0.335\ mm$, by applying Eq(4), $T_n = 5.55\ kN.m$ (for G-Lap300T150)

Table 8. Torsional strength (Theoretical vs Experimental)

No.	Specimen	T_uEXP	Tu ACI(ACI318-19)	Difference ratio (%) with respect to experimental
1	G-Contineous	9.52	8.33	-12.50
2	G-Lap300	8.22	8.33	1.34
3	G-Lap200	6.40	8.33	30.16
4	G-Lap200C	6.93	8.33	20.20
5	G-Lap100	6.05	8.33	37.69
6	G-Lap100C	7.30	8.33	14.11
7	G-Lap300T150	6.98	5.55	-20.49

Table 8 below explains the torsional strength from experimental and ACI318-19 equation. The theoretical value of torsional strength is 8.33 kN·m for all specimens except the G-Lap300T150, which was 5.55 kN·m. The difference ratio for the continuous bar, lap 300, and strengthened beams within splice region was less than or equal to ±20%. The high divergence was observed in specimens with shorter lap splice length (i.e., G-Lap100 and G-Lap200). In this case, the ACI

equation appears to be invalid with the shortest lap splice length (100 and 200 m) due to premature bond-related effects.

6. Conclusion

The present investigation utilized an innovative splice remedy method to fix the issue of inadequate lap splices in reinforced concrete beams tested for pure torque. The experimental results justify a number of conclusions:

- The minimum inadequate lap splice length significantly reduced the torsional load capacity, leading to a loss of up to 36.45% in ultimate torque. The reduction is mainly attributable to inadequate bond strength between the overlapped bars, resulting in early slippage and restricting the efficient transfer of loads due to torsional effect over the splice region. As a result, the beam demonstrated an initial reduction in stiffness and a brittle failure mode.
- The torsional ductility and toughness diminished by 36.76% and 70.7%, respectively, in comparison to the beam with no splice region (continuous reinforcement). The substantial decrease in toughness signifies diminished energy absorption capability, attributed to the initial and rapid progression of splitting cracks at the splice zone.
- Increasing the stirrup spacing in the splice region from 100 mm to 150 mm led to a 15% decrease in ultimate torque capacity. This modification had a negligible effect on ductility and toughness, indicating that although transverse reinforcement offers some confinement, it cannot entirely mitigate the inadequate bond linked to short splices.
- The CFRPsheet wrapped directly around the spliced bars prior to concrete casting improved torque capacity, ductility, and toughness. The enhancement results from the enhanced bond and confinement afforded by the incorporated CFRP, which diminished bar slide and postponed cracking, resulting in an enhanced ductile torsional performance.
- The proposed method is simple and practical, and requires no specialist apparatus such as welding or couplers, providing it an efficient and cost-effective alternative for strengthening reinforced concrete beams with inadequate lap splices.
- Overall, strengthening substandard lap splices using CFRP significantly improves torsional behavior, torsional ductility, and energy absorption, resulting in a safer and more desirable failure mode. This strengthening technique may result in a reduce in the needed lap splice length addition to achieving acceptable torsional strength and safety margins.
- The current test was limited to pure torsional loading on a constant cross-section, missing the ability to apply both bending-torsion loads.
- Future studies should incorporate the effects of combination bending and torsion while varying the concrete cover, as it may considerably affect bond integrity and splice efficiency.
- In addition, as long-term effects may change splice behavior, future research might include durability or cyclic torsion studies.

Acknowledgement

The authors acknowledge their deep thanks to the staff of the College of Engineering, University of Anbar, for their assistance during this work.

References

[1] Hu X, Xue W, Xue W. Bond properties of GFRP rebars in UHPC under different types of test. Eng Struct. 2024;314:118319. https://doi.org/10.1016/j.engstruct.2024.118319

[2] Saleh Z, Goldston M, Remennikov AM, Sheikh MN. Flexural design of GFRP bar reinforced concrete beams: An appraisal of code recommendations. J Build Eng. 2019;25:100794. https://doi.org/10.1016/j.jobe.2019.100794

[3] Bai H, Jiang J, Xue W, Hu X. Experimental investigation on pure torsion behavior of concrete beams reinforced with glass fiber-reinforced polymer bars. Buildings. 2024;14(9):2617. https://doi.org/10.3390/buildings14092617

[4] Ali ZM, Mahmoud AS, Mohammed MS, Ahmed ML. Structural behavior of voided reinforced concrete beams having a novel tact bundled waste plastic bottles. Innov Infrastruct Solut. 2023;8(9):237. https://doi.org/10.1007/s41062-023-01205-7

[5] Panchacharam S, Belarbi A. Torsional behavior of reinforced concrete beams strengthened with FRP composites. In: First FIB Congress. Osaka, Japan; 2002. Vol. 1. p. 1-110.
[6] Abdoli M, Mostofinejad D. Torsional behavior of FRP-strengthened reinforced concrete members considering various wrapping configurations: Theoretical analysis and modeling. Constr Build Mater. 2023;401:132636. https://doi.org/10.1016/j.conbuildmat.2023.132636
[7] Said M, Salah A, Erfan A, Esam A. Experimental analysis of torsional behavior of hybrid fiber reinforced concrete beams. J Build Eng. 2023;71:106574. https://doi.org/10.1016/j.jobe.2023.106574
[8] Shehab HK, El-Awady ME, Husain M, Mandour. Behavior of concrete beams reinforced by FRP bars under torsion. In: 13th Int. Conf. on Soft Ground Engineering. Ain Shams Univ; 2009. p. 931-942.
[9] Deifalla A, Awad A, Elgarhy M. Effectiveness of externally bonded CFRP strips for strengthening flanged beams under torsion: An experimental study. Eng Struct. 2013;56:2065-2075. https://doi.org/10.1016/j.engstruct.2013.08.027
[10] Mohamed HM, Chaallal O, Benmokrane B. Torsional moment capacity and failure mode mechanisms of concrete beams reinforced with carbon FRP bars and stirrups. J Compos Constr. 2015;19(2):1-10. https://doi.org/10.1061/(ASCE)CC.1943-5614.0000515
[11] Mahmoud AS, Ali ZM, Faisal MG. Novel method for strengthening insufficient steel reinforcement splice using CFRP sheets. Int J Comput Aided Eng Technol. 2022;17(1):109-119. https://doi.org/10.1504/IJCAET.2022.124533
[12] Jaffal AN, Hilal AA, Mahmoud AS. Effect of CFRP sheets strengthening method on behaviour of modified lightweight foamed concrete beams. J Eng. 2024;2024(1):5599688. https://doi.org/10.1155/je/5599688
[13] Mahmoud AS, Ali ZM. Behaviour of reinforced GFRP bars concrete beams having strengthened splices using CFRP sheets. Adv Struct Eng. 2021;24:13694332211001516. https://doi.org/10.1177/13694332211001515
[14] Ali ZM, Mahmoud AS, Al-Ani MM. Ductility, stiffness and toughness of modified spliced steel reinforced concrete. In: AIP Conference Proceedings. 2022. Vol. 2386(1). https://doi.org/10.1063/5.0067147
[15] Jassim MK, Mahmoud AS, Mohana MH. Performance of GFRP spliced rebars in self-compacting concrete beams using a new CFRP sheets strengthening technique. Innov Infrastruct Solut. 2025;10(8):366. https://doi.org/10.1007/s41062-025-02163-y
[16] Al-Mamory ZK, Al-Ahmed AHA. Behavior of steel fiber reinforced concrete beams with CFRP wrapped lap splice bars. Structures. 2022;44:1995-2011. https://doi.org/10.1016/j.istruc.2022.08.096
[17] Chao S-H, Naaman AE, Parra-Montesinos GJ. Bond behavior of reinforcing bars in tensile strain-hardening fiber-reinforced cement composites. ACI Struct J. 2009;106(6):897. https://doi.org/10.14359/51663191
[18] Mohammed MS, Ahmed ML, Ali ZM, Mahmoud AS. An innovative method of voided reinforced concrete one-way slabs using bundled waste PET bottled tubes. Mater Sci Forum. 2020;1007:76-84. https://doi.org/10.4028/www.scientific.net/MSF.1007.76